Nanoscale Res Lett (2009) 4:1475–1480
DOI 10.1007/s11671-009-9423-6

NANO EXPRESS

Ultrafast Dynamics of Localized and Delocalized Polaron Transitions in P3HT/PCBM Blend Materials: The Effects of PCBM Concentration

Emmanouil Lioudakis · Ioannis Alexandrou · Andreas Othonos

Received: 9 June 2009 / Accepted: 18 August 2009 / Published online: 3 September 2009

Abstract Nowadays, organic solar cells have the interest of engineers for manufacturing flexible and low cost devices. The considerable progress of this nanotechnology area presents the possibility of investigating new effects from a fundamental science point of view. In this letter we highlight the influence of the concentration of fullerene molecules on the ultrafast transport properties of charged electrons and polarons in P3HT/PCBM blended materials which are crucial for the development of organic solar cells. Especially, we report on the femtosecond dynamics of localized (P_2 at 1.45 eV) and delocalized (DP_2 at 1.76 eV) polaron states of P3HT matrix with the addition of fullerene molecules as well as the free-electron relaxation dynamics of PCBM-related states. Our study shows that as PCBM concentration increases, the amplified exciton dissociation at bulk heterojunctions leads to increased polaron lifetimes. However, the increase in PCBM concentration can be directly related to the localization of polarons, creating thus two competing trends within the material. Our methodology shows that the effect of changes in structure and/or composition can be monitored at the fundamental level toward optimization of device efficiency.

E. Lioudakis (✉)
Energy, Environment and Water Research Center, The Cyprus Institute, P.O. Box 27456, 1645 Nicosia, Cyprus
e-mail: m.lioudakis@cyi.ac.cy

I. Alexandrou
Electrical Engineering and Electronics, University of Liverpool, Liverpool L69 3GJ, UK
e-mail: ioannis@liv.ac.uk

A. Othonos
Research Center of Ultrafast Science, Department of Physics, University of Cyprus, P.O. Box 20537, 1678 Nicosia, Cyprus

Keywords Ultrafast · Composites · Fullerenes · Polarons

The conversion of solar energy into electrical energy using thin film organic photovoltaics has showed great potential as a renewable energy source [1, 2]. Typical organic solar cells are based on the dissociation of photogenerated excitons (electron–hole pairs) by the sunlight to charged carriers and polarons (carriers coupled with the induced polarized electric field) at the vicinity of bulk heterojunctions formed within blends of organic semiconductors [3]. Nowadays, there is good progress toward efficient polymer-based solar cells, and efficiencies of approximately 5% have already been demonstrated [4]. Considerable attention has been focused on high solar efficiency blend materials such as π-conjugated poly-3-hexyl thiophene (P3HT) and fullerene derivatives such as [6,6]-phenyl-C_{61} butyric acid methyl ester (PCBM). Recently, localized and delocalized polaron transitions inside the gap of P3HT matrix were investigated using spectroscopic measurements [5]. Although recent studies on P3HT/PCBM composites have revealed the effect of structural changes on the device efficiency [4], spectroscopic studies of ultrafast electron transfer in these donor–acceptor systems remain a challenge [6, 7].

In this letter, we have investigated the influence of PCBM concentration on the ultrafast photoinduced absorption (PA) of P3HT/PCBM blends after excitation with photon energies large enough to induce excitons in both materials. Our study elucidates the ultrafast polaron dynamics at localized and delocalized polaron transitions of P3HT before and after the dissociation of bound excitons at bulk P3HT/PCBM heterojunctions. Importantly, our ultrafast study also reveals information about the influence

of coupling coefficients and the carrier density present in the localized and delocalized polaron states for materials with different PCBM concentrations. We also present the dynamics of excited states formed at PCBM network chains. We have found that these ultrafast carrier dynamics play the key role in the optimization of carrier transport in these organic solar cells.

Our study utilizes ultrafast spectroscopy with femtosecond resolution (~150 fs) [8] on P3HT/PCBM blend materials with PCBM concentration ranging between 1 and 50 wt%. The utilized materials were fabricated under ambient conditions. P3HT and PCBM were individually dispersed in dichlorobenzene at dissolution ratio of 5 mg per 10 mL of solvent. Both solutions were gently steered over a hot plate (<45 °C) until all solid material was dissolved. Composites were prepared by mixing appropriate amounts of the two solutions inside 1.5 mL vials. The composites were steered in an ultrasonic bath for at least 10 min before drop casting composite layers on quartz substrates. We used identical round quartz substrates and 0.25 mL of composite solution; ensuring thus that the layers have similar thickness[1]. A schematic representation of the utilized blend materials drop casting on quartz substrate is shown in the Fig. 1a. The utilized source for the photoexcitation in this study consists of a self mode-locked Ti:Sapphire oscillator generating 50 fs pulses at 800 nm. A chirped pulsed laser amplifier based on a regenerative cavity configuration is used to amplify the pulses to approximately 2.5 mJ at a repetition rate of 5 kHz. Part of the energy was used to pump an optical parametric amplifier (OPA) for generating UV ultrashort pulses, and a second part of the energy was used to frequency double the fundamental to 400 nm using a non-linear BBO crystal. A half wave plate and a polarizer in front of the non-linear crystal were utilized to control the intensity of the pump incident on the sample. A small part of the fundamental energy was also used to generate a supercontinuum white light by focusing the beam on a sapphire plate. An ultrathin high reflector at 800 nm was used to reject the residual fundamental light from the generated white light to eliminate the possibility of effects by the probe light. The white light probe beam is used in a non-collinear geometry, in a pump–probe configuration where the pump beam was generated from the OPA. Optical elements such as focusing mirrors were utilized to minimize dispersion effects and thus not broadening the

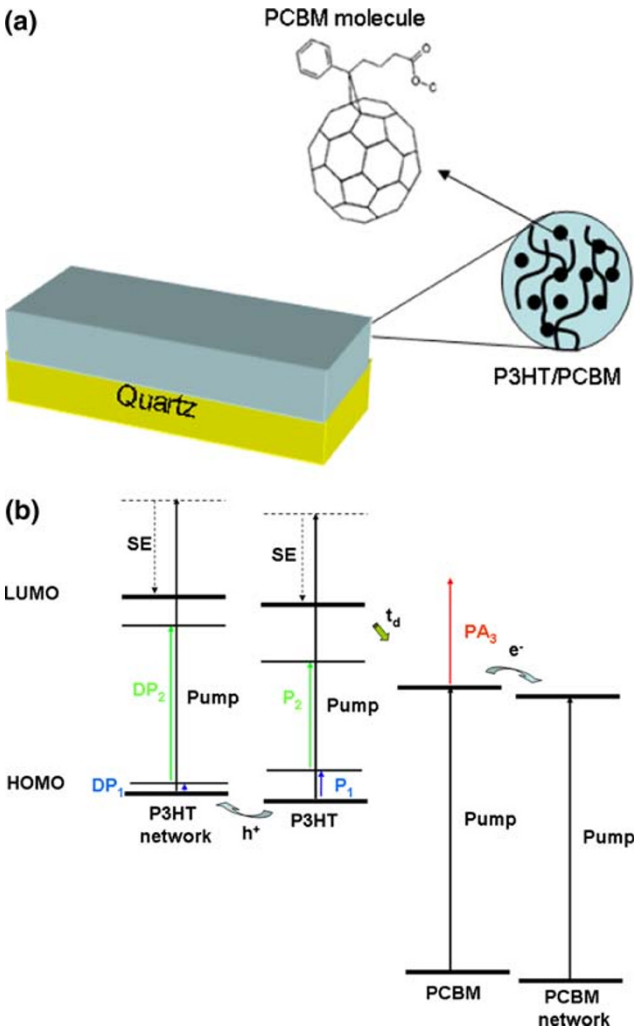

Fig. 1 **a** A schematic representation of the P3HT/PCBM blend materials on the quartz substrate. The zoom shows the morphology of this bulk heterojunctions and the *arrow* indicates the molecular structure of the PCBM. **b** Energy band diagram of blend materials for bound and mobile electrons and holes. The *arrows* P_1 and P_2 represent the localized polarons whereas the DP_1 and DP_2 represent the delocalized polarons, respectively. PA_3 represents the secondary excitation of free electrons in the PCBM and SE the stimulated emission

laser pulse. The reflected and transmission beams are separately directed onto their respective silicon detectors after passing through a band pass filter selecting the probe wavelength from the white light. The differential reflected and transmission signals were measured using lock-in amplifiers with reference to the optical chopper frequency of the pump beam. The temporal variation in the PA signal is extracted using the transient reflection and transmission measurements, which is a direct measure of the photoexcited carrier dynamics within the probing region [9].

Figure 2 shows the transient absorption spectra for 1, 10, and 50 wt% PCBM concentration measured at 0, 1, 2, 10, 100, and 200 ps, following photoexcitation at 3.8 eV.

[1] All our films were prepared from solutions that contain the same concentration of total polymer (P3HT + PCBM) and the same amount of 250 μL of solution was drop cast on identical quartz disks. Therefore, by keeping the mass content and thickness of our films the same through our samples, differences in the absolute value of transient absorption in Fig. 2 can be taken as indication of polaron densities within the material

It is well-known that in this system exciton dissociation happens within a few fs whereas the resolution of our system is pulse-width limited (~150 fs) and therefore our measurements at 0 ps time are possibly affected by charged carriers generated from exciton dissociation. The transient spectra for all samples are consistent with the existence of two PA bands close to the P_2 and DP_2 polaron transitions reported previously [10]. The first band originates from localized polarons in the disordered P3HT regions whereas the second band originates from delocalized polarons in the ordered P3HT regions. A schematic representation of the energy band diagram of this P3HT/PCBM bulk-heterojunction is shown in the Fig. 1b where the optically allowed transitions arising from polarons in P3HT matrix are assigned. Our transient absorption spectra (Fig. 2) are well-described by two superimposing Gaussians centered at 1.45 and 1.76 eV which represent the PA bands of localized and delocalized polarons P_2 and DP_2, respectively [5, 10]. The localized polaron transition P_1 and the delocalized polaron transition DP_1 with energies 0.37 and 0.06 eV, respectively, were investigated elsewhere [5] but are outside the probed energy range in our study.

The experimental data for the 1 wt% PCBM blend show that photoexcited P_2 and DP_2 polarons have a very short relaxation time (within ~100 ps). Similar spectra behavior and relaxation times have also been observed for the pure P3HT polymer matrix [10] which is reasonable since the PCBM concentration in our sample is very low. These PA bands remain at the same energies for all delay times except for a small energy shift (indicated with the horizontal arrows in Fig. 2a) of PA bands between 0 and 1 ps. This is a trend that does not appear in the data for any of the other composites we studied. When the ratio of absorption amplitudes for the P_2 and DP_2 bands is examined as a function of PCBM concentration, an interesting trend is observed. At 1 wt% PCBM the DP_2 transition is stronger with a DP_2 to P_2 ratio of (3:2). This ratio is maintained for all time frames until these polarons relax. With increasing the PCBM concentration to 10 wt%, both absorption amplitudes increase and the DP_2 to P_2 ratio changes to (1:1). At the highest PCBM concentration composite (50 wt%), the absorption amplitudes increase considerably compared to the 1 wt% PCBM blend: P_2 transition becomes ~5.6 times higher while the DP_2 transition increases only by ~1.76 times. As a result the DP_2 to P_2 ratio reduces further to (1:2). The progressive reduction in the DP_2 to P_2 ratio suggests that as the PCBM concentration increases, the P3HT regions with long range order become less, giving rise to disordered regions. Therefore, the introduction of PCBM within the P3HT matrix interrupts P3HT crystallinity which is reasonable

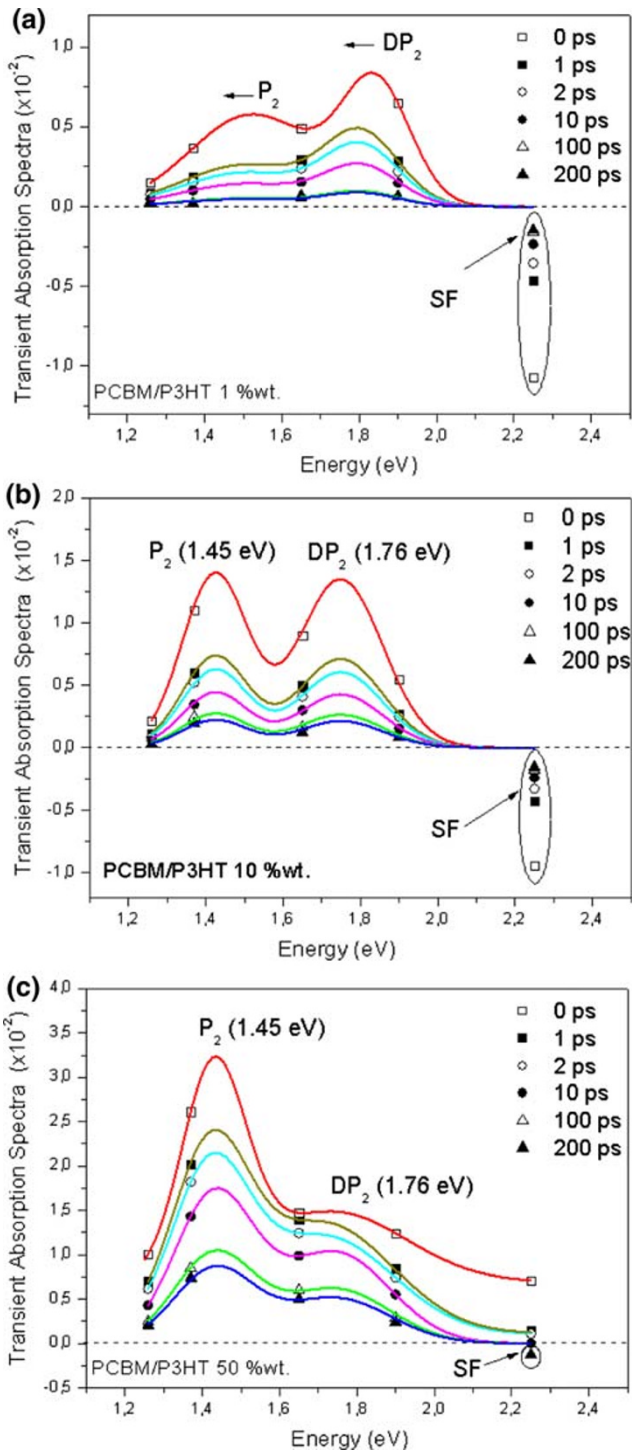

Fig. 2 Transient absorption spectra for P3HT/PCBM blend materials with 1 (**a**), 10 (**b**), and 50 wt% (**c**) PCBM concentration. The spectra measured at 0 ps (*open squares*), 1 ps (*full squares*), 2 ps (*open circles*), 10 ps (*full circles*), 100 ps (*open triangles*), and 200 ps (*full triangles*), respectively, following the pulse excitation at 3.8 eV. The P_2, DP_2, and SF bands are assigned. The color curves represent the fits using a superposition of two Gaussian peaks centered at the reported values of polaron states in the literature [5]

consequence of blending the two materials. However, these results illustrate that the average hole diffusion length will decrease with an expected negative knock on effect on device efficiency.

Another important trend revealed by our data is the increase in lifetime of polarons in P_2 and DP_2 states with increasing the PCBM concentration. The transient absorption spectra of the composite with the highest PCBM concentration show that after 200 ps a similar amount of polarons are still available as in the 1 wt% PCBM composite immediately after (0 ps) the absorption of the pump pulse. In this comparison we also probe an opposite behavior of relative amplitudes for the P_2 and DP_2 polarons between the two samples. Assuming that the fundamental polaron relaxation lifetime for P3HT does not change with increasing PCBM concentration, this trend can be explained by the independent or combined action of increased production of polarons and/or reduced availability of electrons for recombination. The dissociation of excitons formed at the P3HT–PCBM interface is more likely than in bulk P3HT due to the existence of a build-in electric field at the heterojunction. Therefore, as the PCBM concentration increases so does the proportion of excitons that dissociate, resulting in a progressively increasing number of P_2 and DP_2 polarons immediately after the absorption of the pump pulse as can be seen from the relative amplitudes of the spectra in Fig. 2. In addition to increasing the exciton dissociation rate, electron capture by PCBM also minimizes recombination [6]. Therefore, the rate of recombination loss of polarons will decrease as seen in Fig. 2.

Figure 2 also shows that when the PCBM concentration increases, the population of localized polarons (P_2) increases at the expense of the delocalized ones (DP_2). This trend can be attributed directly to the disruption in the long range order of P3HT chains as the PCBM regions increase in size and number. This finding has immediate relevance to the efficiency of P3HT/PCBM solar cells. Our results show that on one hand the population of polarons increases considerably with the addition of PCBM but, on the other, the relative amount of mobile (delocalized) polarons decreases. Therefore, in terms of device efficiency there will be an upper limit in PCBM concentration with further improvements possible only if long range order in P3HT is maintained.

In order to investigate the transport properties of the mobile charged carriers in the P3HT and PCBM network, we studied the transient dynamics of each observable PA band in our spectrum and compared it with that of the PB band at 2.25 eV. Figure 3 shows the transient absorption decay profiles obtained from the films of P3HT/PCBM blend materials with 1, 10, and 50% PCBM concentration, in a time window of 300 ps. Probing at resonance with the P_2 and DP_2 polaron transitions, we observe that the relaxation dynamics of charged polarons are strongly related to the addition of PCBM molecules and consequently to the PCBM–P3HT interaction. Furthermore, the relaxation dynamic of localized polaron (P_2) transition is slower than that of the delocalized (DP_2) for each composite. Similar results for the transmission decay profiles of localized and delocalized polaron states has been reported by Vardeny et al. [10] at a particular PCBM concentration. With increasing the PCBM concentration (Fig. 3c), the relaxation time of both polaron transitions increases considerably. This result is an alternative way of probing the decrease in recombination loss of polarons due to electron capture by PCBM as explained above. This relaxation dynamic of PCBM-related states has been recently reported by our group to be $\sim$1–2 ns [7] and it is important to point out that this long-live charged carrier transport in the PCBM in combination with the reported electron mobility (2×10^{-3} cm^2/Vs [11]) is important for achieving high solar cell efficiency since it enables maximum collection of the photogenerated charges at the photovoltaic electrodes.

In Fig. 2 we have also observed the existence of a photobleaching (PB) band at 2.25 eV for blends with 1 and 10 wt% PCBM concentration where state filling (SF) effect plays the dominant role. This probing energy corresponds to the first vibronic sideband E_1 of the P3HT material where there is a significant density of states [7, 12]. The transient absorption decay profile of the PB band is also shown in the Fig. 3. From the transient absorption spectra we conclude that the relaxation dynamics of this energy state appear to be governed by two recombination mechanisms (fast and slow component). Upon addition of PCBM molecules, the secondary excitations of the mobile electrons (see PA_3 arrow in Fig. 1b) contribute to the absorption signal giving positive absorption changes within the first few ps (two times higher absorption at 3.8 eV of the highest PCBM concentration sample). As a result, the existence of the PA in the highest PCBM concentration composite (Fig. 2c) at 2.25 eV probing energy is attributed to the secondary re-excitations of electrons from the lower unoccupied molecular orbital (LUMO) of PCBM to higher energy states. At this probing energy of 2.25 eV and after the first 10 ps, we have also the ability to detect the PB band (at the first vibronic sideband of P3HT matrix) where the density of states of P3HT seems to play a dominant role in the carrier dynamics [7]. An additional experimental evident of this free-electron re-excitation can be extracted comparing the sign of the absorption change at 3.8 and 3.1 eV [7] excitation using the same probing energy of 2.25 eV.

In order to further examine in a qualitative picture the carrier dynamics on these PA bands, a simplified rate equation model was used to fit the experimental data.

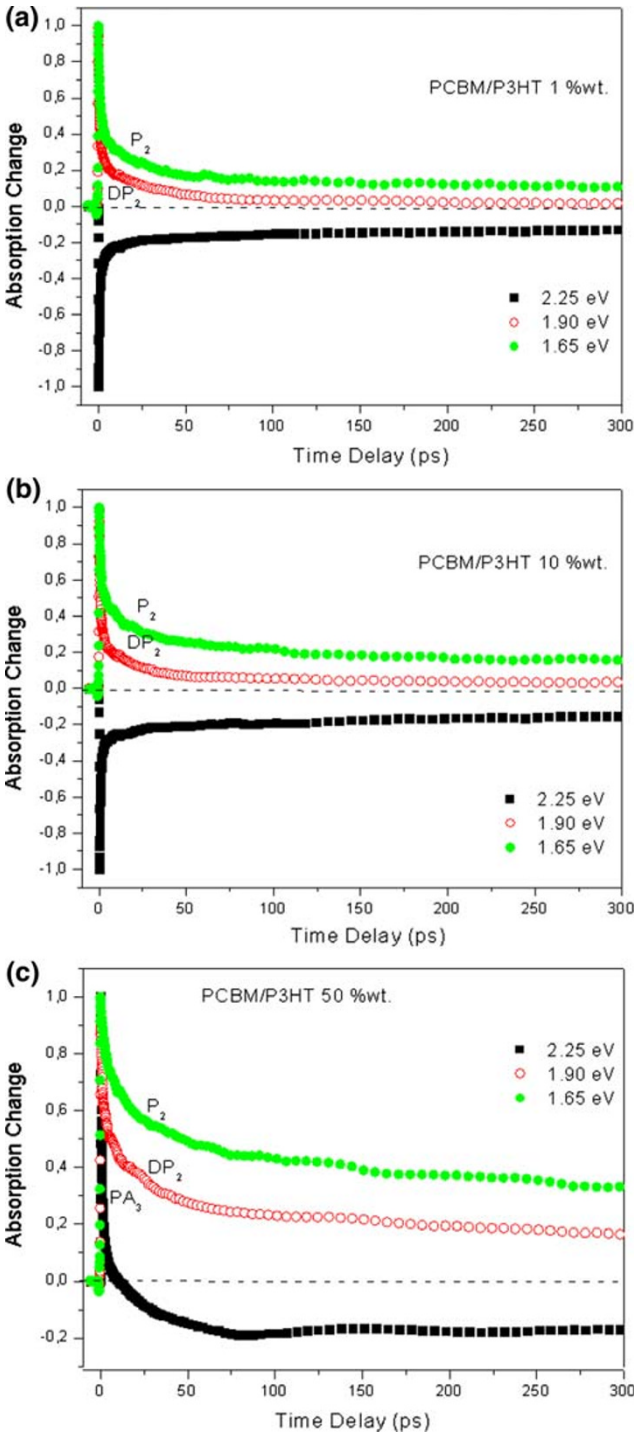

Fig. 3 Transient absorption decay profiles obtained from the films of P3HT/PCBM blend materials with 1 (**a**), 10 (**b**), and 50 wt% (**c**) PCBM concentration probed close to the P_2 and DP_2 bands. The pump energy is 3.8 eV and the excitation fluence 0.5 mJ/cm^2

Following excitation the photogenerated carriers are distributed among various energy states (1, 2,…, n) with characteristic decay time constants τ_1, τ_2,…, τ_n. The temporal changes in absorption are a contribution from all the

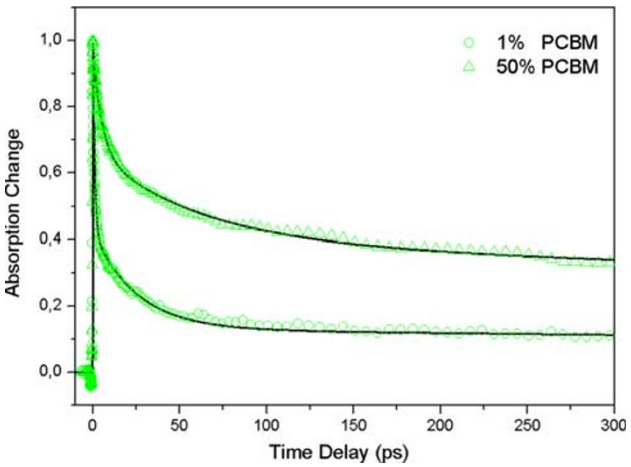

Fig. 4 Transient absorption decay profiles obtained from the films of P3HT/PCBM blend materials with 1 and 50% PCBM concentration probed close to the P_2 band. The pump energy is 3.8 eV and the excitation fluence 0.5 mJ/cm^2. The *solid lines* represent the fitting results of rate equation model using three exponential terms

states. Figure 4 shows the fitting results of this simplified rate equation model on the transient absorption decay profiles of localized polaron transition (P_2) obtained from the P3HT/PCBM blend material with the lowest and highest PCBM concentration. Our data is well fitted using three different relaxation mechanisms/channels for the polarons at the P_2 transition. For the lowest PCBM concentration composite (1 wt%), the first mechanism is very fast (within $\sim$1 ps) and has the higher amplitude contribution (60%) in the absorption signal, the second recovers within 25 ps (30%) and the third has the smaller contribution (10%) with a much slower relaxation time constant ($\sim$2 ns). However, when the same fitting procedure is repeated for the composites with 50 wt% PCBM, the first two relaxation mechanisms become slower (5 and 60 ps, respectively) with the contribution of the first fast mechanism reduced at (34%). The long-live relaxation mechanism has the same time constant $\sim$2 ns but its contribution in the absorption signal increases to 40%. This data confirms that by increasing PCBM concentration polaron recombination is slower and the majority of polaron recombination takes place through the slowest two mechanisms.

Our study shows that there is indeed very close correlation between the structure of the blends and carrier dynamics. As the PCBM concentration increases, so does the availability of polarons in the P3HT matrix. This is expected since exciton dissociation is expected to take place at the P3HT/PCBM heterojunctions. However, we directly probe the gradual decrease in the relative amount of delocalized polarons as the PCBM concentration increases. We would expect that in such devices, as PCBM concentration increases the increased number of polarons find it

progressively more difficult to diffuse within the blends and reach the electrodes. Device annealing has recently been proven to optimize the blend microstructure and improve the device efficiency. Therefore, we can anticipate that by providing direct fundamental information on carrier dynamics our methodology can be used to monitor the effect of blend fabrication steps or post-formation annealing.

References

1. J.Y. Kim, S.H. Kim, H.H. Lee, K. Lee, W. Ma, X. Gong, A.J. Heeger, Adv. Mater. **18**, 572 (2006)
2. H. Hoppe, N.S. Sariciftci, J. Mater. Chem. **16**, 45 (2006)
3. I. Montanari, A.F. Nogueira, J. Nelson, J. Durrant, C. Winder, M.A. Loi, N.S. Sariciftci, C. Brabec, Appl. Phys. Lett. **81**, 3001 (2002)
4. M.R. Reyes, K. Kim, D.L. Carroll, Appl. Phys. Lett. **87**, 083506 (2005)
5. R. Osterbacka, C.P. An, X.M. Jiang, Z.V. Vardeny, Science **839**, 287 (2000)
6. I.-W. Hwang, D. Moses, A.J. Heeger, J. Phys. Chem. C **112**, 4350 (2008)
7. E. Lioudakis, A. Othonos, I. Alexandrou, Y. Hayashi, Appl. Phys. Lett. **91**, 111117 (2007)
8. E. Lioudakis, A.G. Nassiopoulou, A. Othonos, Appl. Phys. Lett. **90**, 171103 (2007)
9. E. Lioudakis, A. Othonos, Phys Stat. Sol. (RRL) **2**, 19 (2008)
10. X.M. Jiang, R. Österbacka, O. Korovyanko, C.P. An, B. Horovitz, R.A.J. Janssen, Z.V. Vardeny, Adv. Funct. Mater. **12**, 587 (2002)
11. V.D. Mihailetchi, J.K.J. van Duren, P.W.M. Blom, J.C. Hummelen, R.A.J. Janssen, J.M. Kroon, M.T. Rispens, W.J.H. Verhees, M.M. Wienk, Adv. Funct. Mater. **13**, 43 (2003)
12. E. Lioudakis, A. Othonos, I. Alexandrou, Y. Hayashi, J. Appl. Phys. **102**, 083104 (2007)